TISSUE ENGINEERING: Part A
Volume 15, Number 2, 2009

DOI: 10.1089/ten.tea.2008.0253

Chondrogenic Differentiation of Adipose-Derived Adult Stem Cells by a Porous Scaffold Derived from Native Articular Cartilage Extracellular Matrix

Nai-Chen Cheng, M.D.,[1,2] Bradley T. Estes, Ph.D.,[1] Hani A. Awad, Ph.D.,[3] and Farshid Guilak, Ph.D.[1]

Adipose-derived adult stem cells (ASCs) have the ability to differentiate into a chondrogenic phenotype in response to specific environmental signals such as growth factors or artificial biomaterial scaffolds. In this study, we examined the hypothesis that a porous scaffold derived exclusively from articular cartilage can induce chondrogenesis of ASCs. Human ASCs were seeded on porous scaffolds derived from adult porcine articular cartilage and cultured in standard medium without exogenous growth factors. Chondrogenesis of ASCs seeded within the scaffold was evident by quantitative RT-PCR analysis for cartilage-specific extracellular matrix (ECM) genes. Histological and immunohistochemical examination showed abundant production of cartilage-specific ECM components—particularly, type II collagen—after 4 or 6 weeks of culture. After 6 weeks of culture, the cellular morphology in the ASC-seeded constructs resembled those in native articular cartilage tissue, with rounded cells residing in the glycosaminoglycan-rich regions of the scaffolds. Biphasic mechanical testing showed that the aggregate modulus of the ASC-seeded constructs increased over time, reaching 150 kPa by day 42, more than threefold higher than that of the unseeded controls. These results suggest that a porous scaffold derived from articular cartilage has the ability to induce chondrogenic differentiation of ASCs without exogenous growth factors, with significant synthesis and accumulation of ECM macromolecules, and the development of mechanical properties approaching those of native cartilage. These findings support the potential for a processed cartilage ECM as a biomaterial scaffold for cartilage tissue engineering. Additional *in vivo* evaluation is necessary to fully recognize the clinical implication of these observations.

Introduction

Cartilage repair or regeneration remains a challenging clinical problem in plastic and orthopedic surgery after tissue damage due to trauma, developmental anomalies, or progressive degeneration such as osteoarthritis. As an avascular tissue with low cellular biosynthetic activity, cartilage has a limited capacity for self-repair.[1] Successful outcomes for articular cartilage lesions have been reported with current treatment options, which include joint lavage, tissue debridement, abrasion arthroplasty, microfracture of the subchondral bone, or the transplantation of autologous or allogeneic osteochondral grafts.[2–13] While these procedures have yielded promising clinical results, many of these approaches can lead to the formation of fibrous tissue, apoptosis, and further cartilage degeneration.[14–16] Currently, one tissue engineering approach, autologous chondrocyte implantation (ACI), has demonstrated positive results in early clinical reports,[17–21] but randomized controlled trials suggest similar efficacy of the ACI procedure compared to the microfracture technique or mosaicplasty.[21,22] While autologous chondrocytes provide a differentiated cell source with significant potential for forming cartilaginous tissue, the isolation of autologous chondrocytes for human use is invasive, requiring a biopsy of what may be otherwise healthy cartilage,[18,23] potentially initiating osteoarthritic changes in the joint.[22,24] Moreover, *in vitro* expansion of chondrocytes is associated with a decreased capacity for chondrogenesis due to dedifferentiation or terminal differentiation of chondrocytes with passaging.[25–28] Some limitations to the ACI procedure may be related to the lack of a scaffold that provides the physical and biological signals required for proper growth and differentiation. Hence, there has been growing interest in determining appropriate combinations of cells, biologically active molecules, and biomaterial scaffolds to promote a strong differentiated phenotype.

[1]Departments of Surgery and Biomedical Engineering, Duke University Medical Center, Durham, North Carolina.
[2]Department of Surgery and Institute of Biomedical Engineering, National Taiwan University, Taipei, Taiwan.
[3]Department of Biomedical Engineering, Center for Musculoskeletal Research, University of Rochester, Rochester, New York.

A number of techniques have been developed for cartilage tissue engineering using primary chondrocytes as a cell source and a variety of biomaterial scaffolds or hydrogels with varying biological and biomechanical properties. Naturally occurring marine-derived biologic biomaterials, such as agarose, alginate, and chitosan, have shown significant promise as scaffolds for cartilage tissue engineering by supporting a chondrocytic phenotype[29–38] but generally have mechanical properties that differ from native cartilage by several orders of magnitude.[39,40] Other combinations of biomaterials have also been used as scaffolds to recreate the unique biochemical and biomechanical characteristics of cartilage, including fibrin,[41] collagen matrix/alginate composites,[42] hyaluronic acid,[43,44] pluronics,[36] polyester elastomers,[45] poly(ethylene glycol),[46,47] and nonwoven porous α-hydroxy esters of polylactic, polyglycolic, and copolymers of the two.[36,45,48,49]

As an alternative source of chondrogenic progenitor cells, adult stem cells derived from a variety of tissues have been investigated for cartilage tissue engineering.[50–53] In particular, recent studies have shown the presence of an abundant source of multipotent adult stem cells that are easily accessible from subcutaneous adipose tissue via liposuction and are capable of chondrogenesis.[54,55] During *in vitro* expansion, adipose-derived stem cells (ASCs) can maintain a stable undifferentiated status without change in telomerase activity over nine passages,[56] suggesting that these cells can be expanded as an abundant cell source without loss of multipotency.[57] ASCs can be induced toward a chondrogenic phenotype by exogenous delivery or genetic overexpression of growth factors, including insulin-like growth factor 1, transforming growth factor-β (TGF-β), and bone morphogenetic protein 6 (BMP-6).[58–62] Nevertheless, the complexities involved in safety and efficacy of either exogenous or genetically induced growth factor delivery have led investigators to examine other mechanisms for inducing chondrogenesis, including physical/chemical factors such as oxygen tension,[50] mechanical stress,[63,64] or biomaterial scaffolds with properties that can support rapid cell growth and differentiation.[65] Such scaffolds include natural and synthetic materials such as collagen, chitosan, silk protein, elastin-like polypeptides, and degradable polymers that influence the growth and differentiation of adult stem cells.[51,52,61,66] A more thorough understanding of the interaction among cells, the biomaterial scaffold, and growth factor signaling will be required for successful cartilage tissue engineering.[67]

In the 1960s, Marshall Urist showed the ability of demineralized bone matrix (DBM) to induce ectopic bone formation, hypothesizing that the active osteoinductive ingredient was BMP.[68] Inspired by this work, we hypothesized that native articular cartilage extracellular matrix (ECM) components may similarly provide signals to drive undifferentiated cells toward chondrogenesis. However, the native cartilage ECM is a dense connective tissue, consisting of a highly organized network of collagen (mostly type II) and large aggregating proteoglycans (i.e., aggrecan), and is characterized by an effective pore size of only a few nanometers,[69] effectively preventing any cellular infiltration. To overcome these limitations, we devised a new process to form a porous, interconnected scaffold derived solely from physical processing of articular cartilage. The goal of this study was to examine the hypothesis that native, devitalized cartilage ECM can induce the chondrogenic differentiation of adult stem cells. The scaffolds were seeded with human ASCs and cultured *in vitro* for 4 or 6 weeks, and analyzed for chondrogenesis by histology, immunohistochemistry, and real-time RT-PCR for cartilage-specific ECM genes. Biphasic mechanical testing was used to measure the aggregate modulus and hydraulic permeability of the tissue-engineered cartilage constructs over the culture period.

Materials and Methods

Preparation of scaffolds

Full-thickness porcine cartilage was harvested from femoral condyles of porcine knee joints ($n = 5$) immediately after sacrifice and finely minced using scalpels. The minced particles were suspended in distilled water (dH_2O) and homogenized using a tissue homogenizer to form a cartilage slurry. The homogenized tissue suspension was centrifuged, the supernatant was removed, and the precipitate tissue particles were resuspended in dH_2O. Aliquots (0.75 mL) of the slurry were placed in wells of a 48-well plate, frozen overnight at $-80^{\circ}C$, and then lyophilized for 24 h. The resulting sponge-like scaffolds were cut using a biopsy punch and scalpel to form constructs 6 mm in diameter by ~ 1.5 mm thick (Fig. 1). These specimens were sterilized using ethylene oxide and outgassed for 1 week before use.

Porosity

The porosity of the unseeded scaffolds was determined quantitatively by two methods, liquid displacement[70] and microCT imaging. Briefly, scaffolds were scanned using a VivaCT40 (SCANCO Medical AG, Basserdorf, Switzerland). High-resolution (10.5 μm) scans with X-ray settings of 55 kVp

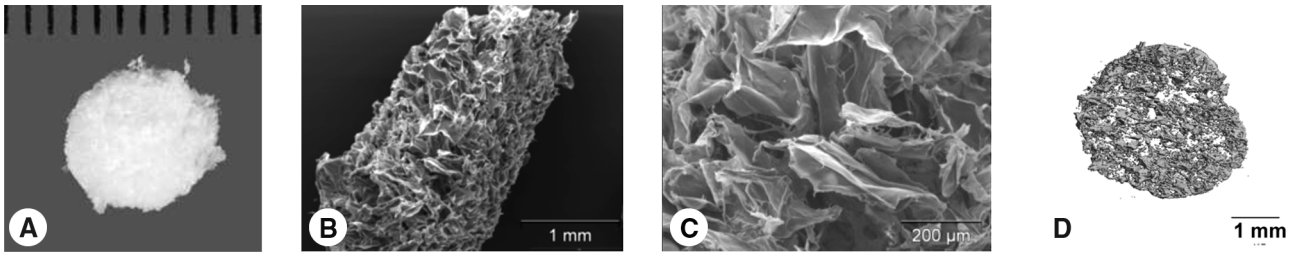

FIG. 1. (**A**) Gross morphology of the porous cartilage–derived matrix. Low (**B**) and high (**C**) magnification SEM images and (**D**) three-dimensional microCT-based rendering of the scaffold demonstrate the porosity of the ECM-derived scaffold.

and 145 μA, an integration time of 600 ms, and a cone beam reconstruction algorithm were used to image the scaffolds. Approximately 80 slices (~0.85 mm thick) of the scaffolds were scanned. The scaffold images were thresholded and analyzed to determine the porosity (%), strut thickness (mm), strut number (1/mm), and pore diameter (mm).

Liquid displacement analysis was also used as an independent measure of specimen porosity.[70] Briefly, dry scaffolds were placed into a known volume (V_1) of hexane in a graduated cylinder. The volume in the cylinder with the scaffolds was then measured, V_2. After 5 min, the hexane impregnated scaffolds were removed, and the volume remaining in the graduated cylinder was measured, V_3. For accurate volumetric readings, images of the graduated cylinder were captured using a high-resolution professional black-and-white video camera (Sony XCD-X700). The volume in the cylinder was calculated by optically measuring the change in meniscus height and then converting to volumetric units using LabView (National Instruments, Austin, TX). The total volume of the scaffold was determined by the following equation:

$$V = (V_2 - V_1) + (V_1 - V_3)$$

where $V_2 - V_1$ equals the dry volume of the scaffold, and $V_1 - V_3$ equals the volume of hexane retained by the scaffold. The porosity of the scaffold was then determined by the ratio of the volume of hexane remaining in the scaffold after removal from the graduated cylinder ($V_1 - V_3$) to the total volume of the scaffold ($V_2 - V_3$).

$$\text{Porosity}\,(\%) = \left(\frac{V_1 - V_3}{V_2 - V_3}\right) \times 100$$

Specimens were also examined by scanning electron microscopy (SEM). Briefly, freeze-dried samples were fixed in 2.5% glutaraldehyde in a 0.1 M sodium cacodylate buffer for 1 h followed by dehydration in a graded series of ethanol washes. The specimens were critical-point dried in CO_2 and then sputter coated with gold. The prepared scaffolds were then viewed with a Philips 501 scanning electron microscope.

Cell culture

Human ASCs were obtained from liposuction waste of subcutaneous adipose tissue from a combination of seven different nonsmoking, nondiabetic female donors with an average age of 41 years (range 27–51) and an average body mass index of 25.17 (range 22.5–28.2) (Zen-Bio, Durham, NC). The cells were cultured separately initially after isolation to ensure similar growth kinetics before the pooling of the cells at passage 1. The cells were plated on 225-cm^2 culture flasks (Corning, Corning, NY) at an initial density of 8000 cells/cm^2 in expansion medium consisting of Dulbecco's modified Eagle's medium (DMEM)–F-12 (Cambrex Bio Science, Walkersville, MD), 10% fetal bovine serum (FBS) (Atlas Biologicals, Ft. Collins, CO), 1% penicillin–streptomycin–Fungizone (Gibco, Grand Island, NY), 0.25 ng/mL TGF-β1 (R&D Systems, Minneapolis, MN), 5 ng/mL epidermal growth factor (Roche Diagnostics, Indianapolis, IN), and 1 ng/mL basic fibroblast growth factor (bFGF or FGF-2) (Roche Diagnostics). The cells were cultured at 37°C in 5% CO_2, and the media were changed every 48 h. When the cells reached 90% confluence, the cells were lifted with 0.05% trypsin and replated. The ASCs were passaged four times, at which point they were trypsinized and counted with a hemocytometer. The cells were resuspended in culture medium at 500,000 cells per 30 μL and seeded by pipetting 30 μL directly on the scaffolds, which were placed in 24-well low-attachment plates (Corning). The culture medium consisted of DMEM-high glucose (Gibco), 10% FBS (Atlas Biologicals), 1% penicillin–streptomycin (Gibco), L-ascorbic acid 2-phosphate (37.5 μg/mL) (Sigma, St. Louis, MO), 1% ITS+ Premix (Collaborative Biomedical; Becton Dickinson, Bedford, MA), and 100 nM dexamethasone (Sigma). At no time point were exogenous growth factors added to the culture medium. The constructs were incubated at 37°C for 1 h to allow the cells to diffuse into and attach to the scaffolds before adding 1 mL of culture medium in each well. The medium was changed every 2–3 days. Cultures were terminated at defined time points during the study for evaluation of chondrogenesis.

RNA isolation and real-time quantitative RT-PCR (qPCR)

Four fresh constructs per time points (1, 3, 7, and 14 days) were transferred into 2 mL microcentrifuge tubes. Total RNA was isolated using the Aurum Total RNA Mini Kit (Bio-Rad Laboratories, Hercules, CA) according to the manufacturer's protocol. Briefly, the constructs were snap frozen, pulverized, and lysed in the supplied lysis buffer. A QIAshredder spin column (Qiagen, Valencia, CA) was used to homogenize the lysate. Ethanol was added to the homogenized lysate before the samples were purified with a spin column. Total RNA concentration was determined by optical density measurement at 260 nm (OD_{260}) using a spectrophotometer (Nanodrop ND-1000, Wilmington, DE). Once isolated, complementary DNA was synthesized from RNA using the iScript reverse transcriptase kit (Bio-Rad). Using commercially purchased primer probes from Applied Biosystems (Foster City, CA), real-time PCR (iCycler; Bio-Rad) was used to compare transcript levels for five different genes: 18S ribosomal RNA (endogenous control; assay ID Hs99999901_s1), aggrecan (AGC1; assay ID Hs00153936_m1), type I collagen (COL1A1; assay ID Hs00164004_m1), type II collagen (COL2A1; custom assay: FWD primer 5-GAGACAGCATG ACGCCGAG-3; REV primer 5-GCGGATGCTCTCAATCTG GT-3; probe 5-FAM-TGGATGCCACACTCAAGTCCCTCA AC-TAMRA-3),[71] and type X collagen (COL10A1; assay ID Hs00166657_m1). Using plasmids containing the section of the gene of interest (GOI), the standard curve method was used to determine starting transcript quantity (SQ) for each respective gene for each sample. qPCR was run in triplicate for each sample for each gene. Data were analyzed by determining the ratio of SQ for the GOI to SQ for 18s for each sample. This ratio was then normalized to this same quantity for the day 0 samples.

$$\text{Fold difference} = \left(\frac{\left(\frac{SQ_{GOI}}{SQ_{18s}}\right)_{\text{day 1, 3, 7, or 14}}}{\left(\frac{SQ_{GOI}}{SQ_{18s}}\right)_{\text{day 0}}}\right)$$

Histology and immunohistochemistry

For histology and immunohistochemistry, constructs ($n = 2$ per time point) were fixed overnight at 4°C in a solution containing 4% paraformaldehyde in a 100 mM sodium cacodylate buffer (pH 7.4), dehydrated in graded ethanol solutions, embedded in paraffin, cut into 5-μm-thick sections, and mounted on SuperFrost microscope slides (Microm International AG, Volketswil, Switzerland). To stain for sulfated glycosaminoglycans (GAGs), sections were treated with hematoxylin for 3 min, 0.02% fast green for 3 min, and 0.1% aqueous safranin-O solution for 5 min; rinsed with dH_2O; and cleared with xylene. Porcine articular cartilage was used for a positive control. Immunohistochemical analysis was also performed on 5-μm sections, using monoclonal antibodies to type I collagen (ab6308; Abcam, Cambridge, MA), type II collagen (II-II6B3; Developmental Studies Hybridoma Bank, University of Iowa, Iowa City, IA), type X collagen (C7974; Sigma), and chondroitin 4-sulfate (2B6; gift from Dr. Virginia Kraus, Duke University Medical Center). Digest-All (Zymed, South San Francisco, CA) was used for pepsin digestion on sections for type I, II, and X collagens. Sections to be labeled for chondroitin 4-sulfate were treated with trypsin, then with soybean trypsin inhibitor, and then with chondroitinase (all from Sigma). The Histostain-Plus ES kit (Zymed) was used on all sections for serum blocking before secondary antibody labeling (anti-mouse IgG antibody; Sigma Catalog No. B7151), and subsequent linking to horseradish peroxidase. Aminoethyl carbazole (Zymed) was used as the enzyme substrate/chromogen. The appropriate positive controls for each antibody were prepared and examined to ensure antibody specificity (porcine cartilage for type II collagen and chondroitin 4-sulfate, calcified zone of cartilage for type X collagen, and cancellous bone for type I collagen). Negative controls without utilizing primary antibodies were also prepared to rule out nonspecific labeling.

Biochemical analysis

Three constructs per time points (0, 1, 7, 14, 28, and 42 days) were digested by incubating in 1 mL of papain (papain [125 μg/mL; Sigma], 100 mM phosphate buffer, 10 mM cysteine, and 10 mM EDTA, pH 6.3) for 24 h at 65°C. GAG content was determined using bovine chondroitin sulfate as a standard and measuring sample content with the dimethylmethylene blue assay.[72] Total collagen content was determined by measuring the hydroxyproline content of the scaffolds after acid hydrolysis and reaction with *p*-dimethylaminobenzaldehyde and chloramine-T, using 0.134 as the ratio of hydroxyproline to collagen.[73] Both total collagen content and GAG content were normalized to total DNA content, which was measured fluorometrically using the PicoGreen fluorescent double-stranded DNA assay (Molecular Probes, Eugene, OR) according to the manufacturer's protocol (excitation wavelength, 485 nm; emission wavelength, 535 nm).

Mechanical testing

A minimum of five fresh constructs after 28 and 42 days in culture were collected for mechanical testing. Cylindrical plugs were punched from the central regions of the engineered cartilage tissue using a biopsy punch to ensure circular geometries for mechanical testing. Creep experiments were conducted in confined compression[74] using an electromechanical materials testing system (ELF 3200; Bose, Minnetonka, MN). Briefly, specimens were placed in a confining chamber in a PBS bath, and compressive loads were applied using a rigid porous platen. After equilibration of a small tare load (1–5 gf), a step compressive load (5–25 gf dependent on time point such that final equilibrium strain was between 15% and 20%) was applied to the sample and allowed to equilibrate for 2000 s. The compressive aggregate modulus (H_A) and hydraulic permeability (k) were determined using a three-parameter, nonlinear least-squares regression procedure.

Statistical analysis

Analysis of variance (ANOVA) and Fisher's PLSD *post hoc* *t*-test were used to determine the statistical significance of the differences in the experimental readouts between time points ($\alpha = 0.05$).

Results

Scaffold porosity

As determined by liquid displacement analysis, the porosity of the scaffolds was determined to be $96.5 \pm 0.95\%$ (mean ± standard error [SE]) porous ($n = 4$). In close agreement to liquid displacement measurement, microCT analysis revealed a porosity of $94.04 \pm 1.54\%$ (mean ± SE; $n = 5$). We also evaluated the microarchitecture of the scaffolds using microCT. The scaffolds had an average strut number of $4.92 \pm 1.62\ mm^{-1}$ (a stereologic measure of the number of struts in the scaffold tissue that intersect a 1 mm long line), strut thickness of 31 ± 1 μm, and strut spacing (equivalent to average pore size) of 221 ± 54 μm. In agreement with the microCT data, SEM revealed a wide range of pore sizes from approximately 10 to 300 μm with mostly open pore structure (Fig. 1).

Real-time qPCR

The two positive markers for chondrogenesis, AGC1 and COL2A1, and two negative markers for chondrogenesis, COL1A1 and COL10A1, were analyzed (Fig. 2). The two positive markers were significantly upregulated by the scaffold. AGC1 was significantly increased approximately 50-fold relative to day 0 control cells, which persisted through day 14, but this increase was not observed until day 7. COL2A1 transcript values were also significantly upregulated several hundred-fold over the first 7 days to 1600-fold by day 14. No significant differences were observed in COL1A1 transcript levels at all times points examined. A slight trend showing an increase in COL1A1 production was noted through day 7, which had dropped back down to initial values by day 14 ($p > 0.05$). A significant downregulation of COL10A1, a marker of the chondrocyte hypertrophy, was observed. By day 14, COL10A1 levels had decreased approximately threefold relative to day 0 control cells.

Gross morphology, immunohistochemistry, and histology

By day 14, the ASC-seeded scaffolds had become opaque with a smooth, white surface. The scaffolds were approxi-

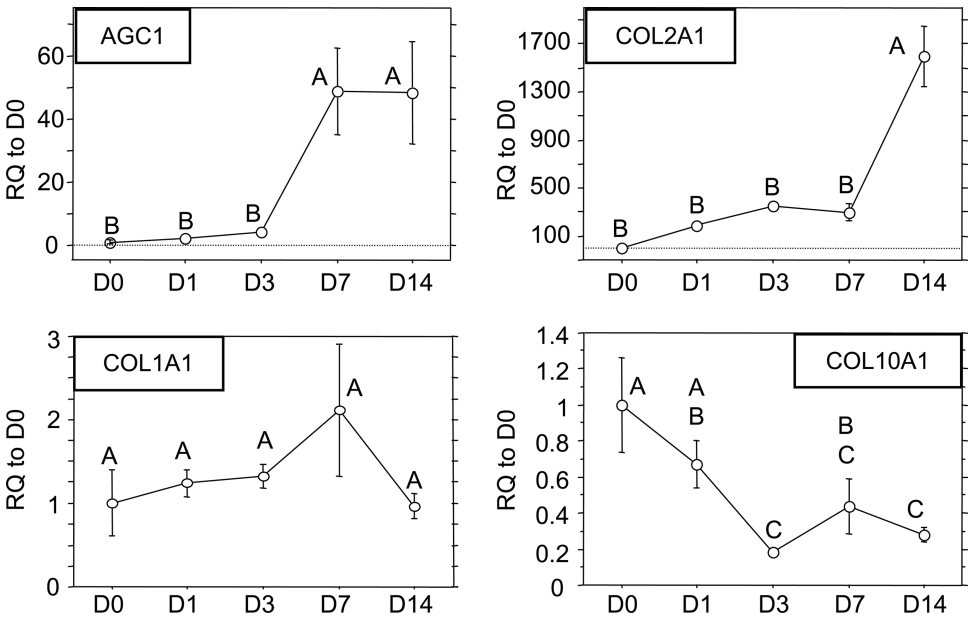

FIG. 2. qPCR results for AGC1, COL2A1, COL1A1, and COL10A1. Data presented as mean ± SE of the relative quantification (RQ) to day 0 transcript values. (Time points not sharing the same letter are statistically different from each other, $p < 0.05$, ANOVA.)

mately the same size through 28 days of culture and appeared to shrink in size from day 28 to 42 (Fig. 3). Significant deposition and accumulation of ECM components within the constructs was evident through immunohistochemical and histological analysis. The sparse, porous scaffold became nearly completely filled with neotissue by day 28 (Fig. 4). Specifically, type II collagen, the primary collagen found in articular cartilage, was found in abundance throughout the matrix interstitial voids and persisted through day 42. In terms of GAG content, immunohistochemistry revealed labeling for the chondroitin 4-sulfate epitope. Total GAG content, as stained by safranin-O, revealed heterogeneous deposition of negatively charged proteoglycans throughout the matrix. Type I collagen, a negative marker for chondrogenesis, was also observed to increase up to day 42. Type X collagen, a cartilage hypertrophic phenotypic marker, was observed within the collagenous matrix at day 28 and diminished significantly by day 42. Of the collagens assayed, type II dominated the composition of the matrix at both day 28 and day 42 time points. High-magnification images (Fig. 4) revealed rounded cells within the matrix that stained for both GAGs (safranin-O) and type II collagen. Conversely, within the interstices between these larger regions of neomatrix, elongated, more fibroblast-like cells were found, which were negative for type II collagen and positive for type I collagen (Fig. 4).

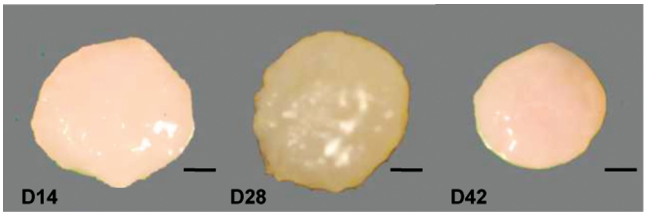

FIG. 3. Gross morphology of the ASC-seeded scaffolds at 14, 28, and 42 days in culture. Some slight contraction of the constructs was observed between days 28 and 42 (scale bar: 1 mm). Color images available online at www.liebertonline.com/ten.

Biochemical analysis

A trend for increasing collagen content (Fig. 5) was noted throughout the experiment, though differences in collagen content were not statistically different (ANOVA; $p = 0.09$). Particularly, from day 7 to 14, collagen content was increased from 115 μg collagen/μg DNA to a value of 136 μg collagen/μg DNA. This content was maintained through the final 28 days of the experiment. GAG content (Fig. 5), conversely, showed a significant decreasing trend throughout the duration of the experiment (ANOVA; $p < 0.0001$). Total GAG content was at its highest at day 1, with a 58% decline in GAG content through day 7. By day 14, GAG content was 30% of the day 1 starting quantity.

Biomechanical testing

The aggregate modulus (Fig. 6) of the scaffolds increased over time (ANOVA; $p < 0.05$) from initial values of 0.041 to 0.079 MPa at day 28, and to 0.151 MPa at day 42 ($p < 0.02$ vs. day 0). The hydraulic permeability (Fig. 6) of the scaffolds showed a trend of decreasing approximately fivefold over the culture period, from $0.33\,mm^4/(N \cdot s)$ at day 0 to $0.055\,mm^4/(N \cdot s)$ at day 42 (ANOVA; $p = 0.44$).

Discussion

The findings of this study show that a porous biomaterial scaffold derived entirely from native cartilage ECM has the ability to induce the chondrogenic differentiation of ASCs without the use of exogenous growth factors. By measures of gene expression, protein synthesis, histology, and biomechanical testing, ASCs produced significant amounts of cartilaginous tissue within the interstitial space of the porous cartilage matrix without additional exogenous growth factors, leading to significant increases in the functional properties of the scaffolds after 4 and 6 weeks of *in vitro* culture.

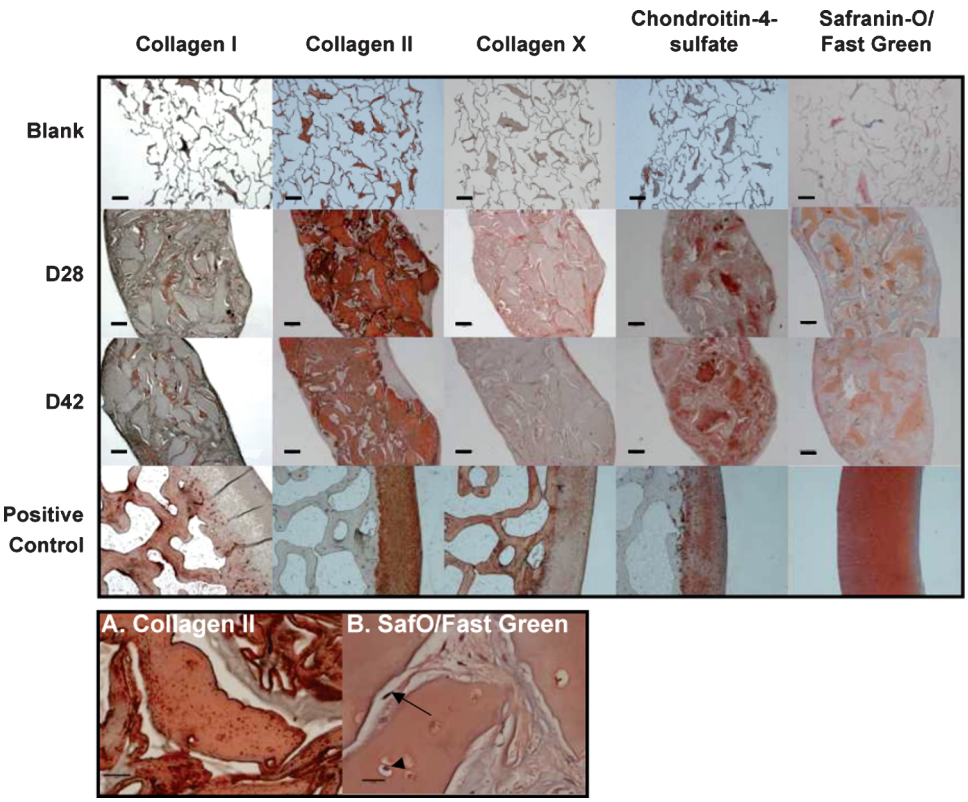

FIG. 4. (Top) Immunohistochemistry/histology of ECM-derived scaffold/ASC cultures. First row: blank scaffolds before seeding. Second row: day 28 samples. Third row: day 42 samples. Fourth row: positive control samples—porcine subchondral bone for type I collagen, porcine cartilage for type II collagen, calcified zone of porcine cartilage for type X collagen, and porcine cartilage for chondroitin 4-sulfate and safranin-O. Scale bar: 200 μm. (Bottom) Day 42 high-magnification images of immunohistochemistry/histology of constructs. (**A**) Type II collagen (II-II6B3) (scale bar: 50 μm) and (**B**) safranin-O/fast green (scale bar: 20 μm). A rounded cell within the matrix (arrowhead) and an elongated, fibroblast-like cell within the neomatrix (arrow) are noted. Color images available online at www.liebertonline.com/ten.

Although the mechanisms leading to the induction of this chondrogenic differentiation remain to be determined, the results suggest that direct cell–matrix interactions significantly influenced the phenotype of ASCs.

An important characteristic of the scaffolds used in this study is the relative simplicity of the processing method (i.e., homogenization and lyophilization) used to fabricate highly porous structures from native cartilage ECM. Recently, decellularized scaffolds derived from a variety of intact tissues have been applied in engineering different tissues or organs, including tendons, ligaments, blood vessels, skin, nerves, skeletal muscle, small intestinal submucosa, urinary bladder, heart, and liver.[75–81] Decellularized and lyophilized osteochondral grafts have also been used successfully to treat full-thickness cartilage lesions in a rabbit model.[82] In the present study, we adopted a relatively simple yet effective method to reconstitute the cartilage tissue into a three-dimensional porous structure with a porosity of ~95% and an interconnected network of pores with an average pore size of 221 μm (Fig. 1). The fact that the scaffold was manufactured using purely physical processing techniques suggests that their native biochemical makeup is likely to be unchanged, which could alleviate safety concerns associated with man-made biomaterial scaffolds. However, the effects of scaffold processing on the matrix biochemistry have yet to be characterized. The porous nature of the scaffolds distinguishes them from traditional cartilage allografts because it facilitates cell seeding. Further, due to the endogenous content of organic ECM molecules and cartilage-derived matrix proteins (CDMPs), we believe that the cartilage-derived ECM scaffolds would be analogous to DBM and similar bone derivatives currently used in bone repair.

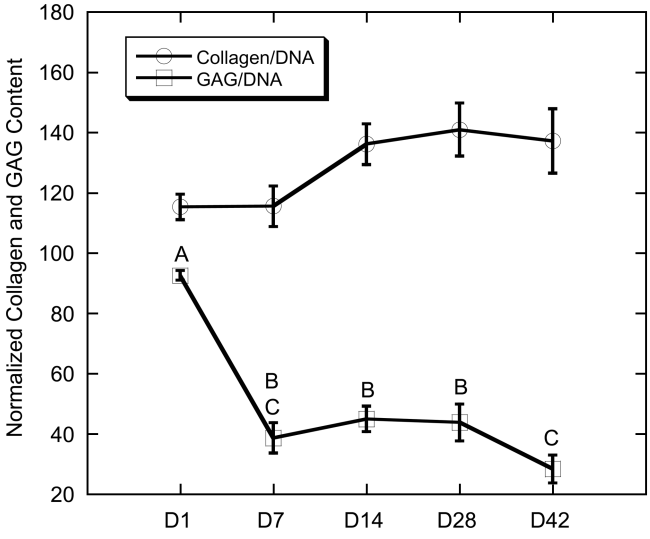

FIG. 5. Total collagen and GAG content normalized to DNA. Data presented as mean ± SE. (Time points not sharing the same letter are statistically different from each other, $p < 0.05$, ANOVA.)

The scaffold induced temporal increases in critical cartilage-specific gene transcripts over the first 14 days of culture, providing evidence of the influence of the scaffold on cell differentiation. In particular, mRNA transcript levels for aggrecan, the large aggregating proteoglycan found in articular cartilage, and type II collagen, the principal collagen found in articular cartilage, were significantly upregulated. These results are comparable to the effects of growth factors

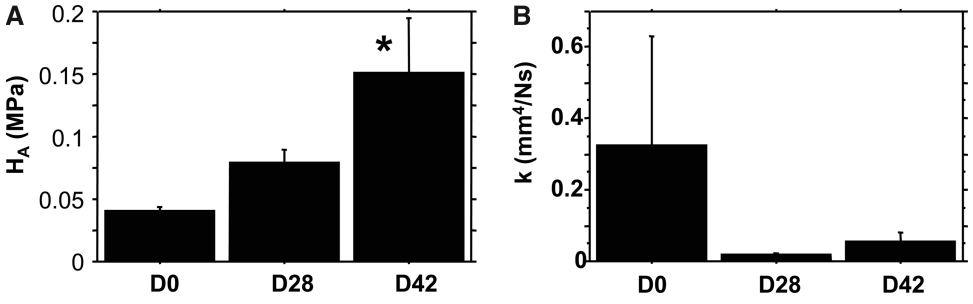

FIG. 6. (**A**) Aggregate modulus (H_A) and (**B**) hydraulic permeability (k) of scaffolds at days 28 and 42. Data presented as mean ± SE. *$p < 0.05$ versus day 0 Control ($n \geq 6$/time point for days 28 and 42). Articular cartilage reference values: $H_A = 500$–900 kPa and $k = \sim 0.005\,\text{mm}^4/(\text{N}\cdot\text{s})$.[86]

that would otherwise be required to induce significant levels of AGC1 and COL2A1 transcripts in these cells.[59,60] Specifically for COL2A1 transcript, ASCs produce little to none of this cartilage-specific transcript in their native environment or even during monolayer expansion, providing further evidence that the scaffold is cueing the cells to produce type II collagen. The paucity of COL2A1 transcript after monolayer expansion combined with significant increases in COL2A1 production directly lead to the 1600-fold increase at day 14 that was observed in this study. The scaffold also inhibited expression of the chondrocyte hypertrophy marker, COL10A1, as has been shown with exogenous BMP-6 treatment.[59]

It is important to note that by histological and immunohistochemical measures, the ASC-seeded scaffolds produced a fibrocartilaginous phenotype as noted by coexpression of type I and II collagen (Fig. 4), though type II collagen dominated the composition. A link between early expression of COL2A1 and type II collagen production was observed (Figs. 2 and 4). However, it should also be noted that ASCs express a high level of COL1A1 at isolation, in the order of 1000-fold higher than that of COL2A1. This level of COL1A1 typically persists through monolayer expansion and increases during differentiation culture.[56,60] Conversely, in this study, a trend toward decreased COL1A1 expression over the first 14 days was observed, which corresponded to significant decreases in type I collagen accumulation in the matrix at days 28 and 42 of culture (Figs. 2 and 4). Type I collagen was primarily located in regions between the larger masses within the neotissue and was associated with a fibroblast-like morphology (Fig. 4) as opposed to the rounded chondrocyte–like morphology observed in the other larger areas of the neotissue. Earlier immunohistochemical time points could elucidate whether a type I collagen phenotype precedes type II collagen deposition within these ECM-derived scaffolds or whether other factors in the scaffold/ASC matrix are implicated in this morphology and collagen phenotype shift. Nonetheless, the fact that the scaffold minimized type I collagen synthesis within each construct as a whole and induced such large quantities of type II collagen indicates that the ASCs are responding to signals and conditions generated from the cartilage-derived scaffold to differentiate to a cartilage phenotype. This significant production of type II collagen at the protein level was encouraging, as the synthesis and assembly of significant amounts of collagen is often considered to be a limiting step in cartilage formation, prompting the search for other means to induce collagen synthesis.[83] Noting the difficulty in synthesizing collagen and the fact that matrix biosynthetic rates are upregulated in injured cartilage,[84] Ng *et al*. suggested that the limiting factor in collagen synthesis is related to the lack of appropriate stimuli to induce rapid tissue remodeling.[83] As exhibited in this study, under appropriate stimulation from the ECM-derived scaffold to the ASCs embedded within the scaffolds, collagen biosynthesis and accumulation was significant in a relatively short culture period.

The biomechanical properties of tissue-engineered cartilage and how they compare to native articular cartilage are among the most important outcome measures in functional tissue engineering.[85] In this study, the biomechanical properties improved progressively over time. The aggregate modulus reached 150 kPa after 42 days in culture (Fig. 6). These values are on the same order of magnitude as those of native articular cartilage (500–900 kPa).[86] These values are also similar to those reported previously for chondrocytes and mesenchymal stem cells (MSCs) encapsulated in agarose.[33,34,87,88] Using articular chondrocytes, these authors obtained aggregate moduli of 100 and 15 kPa after 4 weeks in mechanically stimulated and static culture, respectively,[34] and after 70 days in static culture, the yield equilibrium modulus of chondrocyte-embedded agarose reached 140 kPa compared to MSCs embedded in agarose with a value of 48 kPa.[88] ECM accumulation in the scaffold also decreased the permeability of the constructs by approximately 10-fold from initial values to a value of $0.05\,\text{mm}^4/(\text{N}\cdot\text{s})$ at 42 days, which is approximately 10 times greater than that of native articular cartilage.[89] Interestingly, the improvement in the biomechanical properties was qualitatively associated with the increase in normalized collagen content over time, but seemed to be independent of the temporal changes in GAG content. Because diffusion is considered to be the primary mechanism for macromolecular transport in tissue-engineered cartilage and a rate-limiting factor in scaling up tissue-engineered constructs, providing an adequate nutrient supply may be necessary for enhanced cell proliferation and ECM production,[90] which is likely to further improve the biomechanical properties of these scaffolds. The use of bioreactors to improve nutrient transport, therefore, may be beneficial for further development of the ASC-seeded scaffolds.

We have previously demonstrated that ASCs encapsulated (or suspended) in hydrogel scaffolds (alginate and agarose) produce relatively small amounts of pericelluar and ECM after 28 days in culture under established chondrogenic conditions.[56,58,59,91] These previous results are in contrast to the abundant matrix that we observed with the ECM-derived scaffolds. Further, the chondrogenic differentiation of the ASCs was induced without exogenous growth factors as has previously been required.[56,58,59,91] One possible explanation

is that direct anchorage of the cells to the ECM-derived scaffold may provide cues for cell proliferation and differentiation. Failure to anchor may result in a state of "anoikis" or "homelessness," which, in turn, has been shown to invoke apoptosis in anchorage-dependent cells.[92,93] Not only can failure to provide proper anchorage points result in apoptosis, but failure to provide the proper type of substrate for anchorage can also inhibit differentiation. As evidence of this, chondrogenesis of mouse limb bud MSCs can be inhibited by blocking specific integrins, providing further support of the need of certain types of stem cells to be anchored before differentiation can occur.[94] Larson *et al*. demonstrated that culturing chondrocytes with a native pericellular matrix greatly enhanced the production of ECM macromolecules compared to chondrocytes without a pericellular matrix.[95] Chondrogenesis of MSCs has also been enhanced by culture in type II collagen–based hydrogels, further suggesting that native ECM components, at least in part, guide the differentiation process.[96] Another potential mechanism for the upregulation of ECM production by ASCs may be through the production of "matrikines," or partially broken down matrix macromolecules, as a by-product of the manufacturing process. Matrikines have been shown to have profound effects on cell activity and consequently on matrix synthesis and degradation (reviewed by Maquart *et al*.[97]). The residual, endogenous amounts of active growth factors that remain in the scaffold after processing might also influence the differentiation of the ASCs. Indeed, the potential for scaffolds derived from various native biological tissues to release bioactive factors for both cell proliferation and differentiation has been demonstrated in several recent studies.[77,98] Analogous to the work of Urist,[68] it is possible that growth factors retained in the scaffolds include CDMPs, which may be released by proteolytic degradation of the ECM-derived scaffold or through diffusion and stimulate ASCs down the chondrogenic lineage.[99] Future studies quantifying the biochemical profile and endogenous content of CDMPs in the ECM-derived scaffold, blocking integrin-mediated attachment, and/or investigating specific collagen or peptide sequences may yield additional data on ASC chondrogenesis.

In summary, this study reports the development of a devitalized, cartilage ECM-derived porous scaffold to promote chondrogenesis in ASCs. Our findings support the hypothesis that a scaffold derived from reconstituted cartilage ECM can influence the growth and chondrogenic differentiation of adult stem cells, even in the absence of exogenous growth factors in the culture medium.

Acknowledgments

We would like to acknowledge and thank Stacey Dementoand Matthew W. Hawk for their work in the initial characterization of the ECM-derived scaffold. The II-II6B3 monoclonal antibody developed by Thomas F. Linsenmayer was obtained from the Developmental Studies Hybridoma Bank developed under the auspices of the National Institute of Child Health and Human Development and maintained at The University of Iowa, Iowa City.

Disclosure Statement

No competing financial interests exist.

References

1. Guilak, F., and Hung, C.T. Physical regulation of cartilage metabolism. In: Mow, V.C., and Huiskes, R., eds. Basic Orthopaedic Biomechanics and Mechano-Biology. Philadelphia, PA: Lippincott Williams & Wilkins, pp. 259–300, 2005.
2. Wouters, E., Bassett, F.H., 3rd, Hardaker, W.T., Jr., and Garrett, W.E., Jr. An algorithm for arthroscopy in the over-50 age group. Am J Sports Med **20,** 141, 1992.
3. Denoncourt, P.M., Patel, D., and Dimakopoulos, P. Arthroscopy update #1. Treatment of osteochondrosis dissecans of the knee by arthroscopic curettage, follow-up study. Orthop Rev **15,** 652, 1986.
4. Aichroth, P.M., Patel, D.V., and Moyes, S.T. A prospective review of arthroscopic debridement for degenerative joint disease of the knee. Int Orthop **15,** 351, 1991.
5. Baumgaertner, M.R., Cannon, W.D., Jr., Vittori, J.M., Schmidt, E.S., and Maurer, R.C. Arthroscopic debridement of the arthritic knee. Clin Orthop Relat Res **253,** 197, 1990.
6. Johnson, L.L. Arthroscopic abrasion arthroplasty: a review. Clin Orthop Relat Res, **391 (suppl),** S306, 2001.
7. Friedman, M.J., Berasi, C.C., and Fox, J.M. Preliminary results with abrasion arthroplasty in the osteoarthritic knee. Clin Orthop Relat Res **182,** 200, 1984.
8. Steadman, J.R., Briggs, K.K., Rodrigo, J.J., Kocher, M.S., Gill, T.J., and Rodkey, W.G. Outcomes of microfracture for traumatic chondral defects of the knee: average 11-year follow-up. Arthroscopy **19,** 477, 2003.
9. Steadman, J.R., Rodkey, W.G., and Rodrigo, J.J. Microfracture: surgical technique and rehabilitation to treat chondral defects. Clin Orthop Relat Res **391 (suppl),** S362, 2001.
10. Kish, G., Modis, L., and Hangody, L. Osteochondral mosaicplasty for the treatment of focal chondral and osteochondral lesions of the knee and talus in the athlete. Rationale, indications, techniques, and results. Clin Sports Med **18,** 45, 1999.
11. Aubin, P.P., Cheah, H.K., Davis, A.M., and Gross, A.E. Long-term followup of fresh femoral osteochondral allografts for posttraumatic knee defects. Clin Orthop Relat Res **391 (suppl),** S318, 2001.
12. Emmerson, B.C., Gortz, S., Jamali, A.A., Chung, C., Amiel, D., and Bugbee, W.D. Fresh osteochondral allografting in the treatment of osteochondritis dissecans of the femoral condyle. Am J Sports Med **35,** 907, 2007.
13. Ghazavi, M.T., Pritzker, K.P., Davis, A.M., and Gross, A.E. Fresh osteochondral allografts for post-traumatic osteochondral defects of the knee. J Bone Joint Surg Br **79,** 1008, 1997.
14. Shapiro, F., Koide, S., and Glimcher, M.J. Cell origin and differentiation in the repair of full-thickness defects of articular cartilage. J Bone Joint Surg Am **75,** 532, 1993.
15. Tew, S.R., Kwan, A.P., Hann, A., Thomson, B.M., and Archer, C.W. The reactions of articular cartilage to experimental wounding: role of apoptosis. Arthritis Rheum **43,** 215, 2000.
16. Nehrer, S., Spector, M., and Minas, T. Histologic analysis of tissue after failed cartilage repair procedures. Clin Orthop Relat Res **365,** 149, 1999.
17. Breinan, H.A., Minas, T., Hsu, H.P., Nehrer, S., Sledge, C.B., and Spector, M. Effect of cultured autologous chondrocytes on repair of chondral defects in a canine model. J Bone Joint Surg Am **79,** 1439, 1997.
18. Brittberg, M., Lindahl, A., Nilsson, A., Ohlsson, C., Isaksson, O., and Peterson, L. Treatment of deep cartilage defects in the knee with autologous chondrocyte transplantation. N Engl J Med **331,** 889, 1994.

19. Bentley, G., Biant, L.C., Carrington, R.W., Akmal, M., Goldberg, A., Williams, A.M., Skinner, J.A., and Pringle, J. A prospective, randomised comparison of autologous chondrocyte implantation versus mosaicplasty for osteochondral defects in the knee. J Bone Joint Surg Br **85,** 223, 2003.
20. Minas, T. Autologous chondrocyte implantation for focal chondral defects of the knee. Clin Orthop Relat Res **391,** S349, 2001.
21. Saris, D.B., Vanlauwe, J., Victor, J., Haspl, M., Bohnsack, M., Fortems, Y., Vandekerckhove, B., Almqvist, K.F., Claes, T., Handelberg, F., Lagae, K., van der Bauwhede, J., Vandenneucker, H., Yang, K.G., Jelic, M., Verdonk, R., Veulemans, N., Bellemans, J., and Luyten, F.P. Characterized chondrocyte implantation results in better structural repair when treating symptomatic cartilage defects of the knee in a randomized controlled trial versus microfracture. Am J Sports Med **36,** 235, 2008.
22. Knutsen, G., Engebretsen, L., Ludvigsen, T.C., Drogset, J.O., Grontvedt, T., Solheim, E., Strand, T., Roberts, S., Isaksen, V., and Johansen, O. Autologous chondrocyte implantation compared with microfracture in the knee. A randomized trial. J Bone Joint Surg Am **86-A,** 455, 2004.
23. Kim, H.A., Suh, D.I., and Song, Y.W. Relationship between chondrocyte apoptosis and matrix depletion in human articular cartilage. J Rheumatol **28,** 2038, 2001.
24. Lee, C.R., Grodzinsky, A.J., Hsu, H.P., Martin, S.D., and Spector, M. Effects of harvest and selected cartilage repair procedures on the physical and biochemical properties of articular cartilage in the canine knee. J Orthop Res **18,** 790, 2000.
25. Bonaventure, J., Kadhom, N., Cohen-Solal, L., Ng, K.H., Bourguignon, J., Lasselin, C., and Freisinger, P. Reexpression of cartilage-specific genes by dedifferentiated human articular chondrocytes cultured in alginate beads. Exp Cell Res **212,** 97, 1994.
26. Darling, E.M., and Athanasiou, K.A. Rapid phenotypic changes in passaged articular chondrocyte subpopulations. J Orthop Res **23,** 425, 2005.
27. Stokes, D.G., Liu, G., Coimbra, I.B., Piera-Velazquez, S., Crowl, R.M., and Jimenez, S.A. Assessment of the gene expression profile of differentiated and dedifferentiated human fetal chondrocytes by microarray analysis. Arthritis Rheum **46,** 404, 2002.
28. Thirion, S., and Berenbaum, F. Culture and phenotyping of chondrocytes in primary culture. Methods Mol Med **100,** 1, 2004.
29. Mierisch, C.M., Cohen, S.B., Jordan, L.C., Robertson, P.G., Balian, G., and Diduch, D.R. Transforming growth factor-beta in calcium alginate beads for the treatment of articular cartilage defects in the rabbit. Arthroscopy **18,** 892, 2002.
30. Iwasaki, N., Yamane, S.T., Majima, T., Kasahara, Y., Minami, A., Harada, K., Nonaka, S., Maekawa, N., Tamura, H., Tokura, S., Shiono, M., Monde, K., and Nishimura, S. Feasibility of polysaccharide hybrid materials for scaffolds in cartilage tissue engineering: evaluation of chondrocyte adhesion to polyion complex fibers prepared from alginate and chitosan. Biomacromolecules **5,** 828, 2004.
31. Domm, C., Schunke, M., Steinhagen, J., Freitag, S., and Kurz, B. Influence of various alginate brands on the redifferentiation of dedifferentiated bovine articular chondrocytes in alginate bead culture under high and low oxygen tension. Tissue Eng **10,** 1796, 2004.
32. Buschmann, M.D., Gluzband, Y.A., Grodzinsky, A.J., and Hunziker, E.B. Mechanical compression modulates matrix biosynthesis in chondrocyte/agarose culture. J Cell Sci **108 (Pt 4),** 1497, 1995.
33. Mauck, R.L., Nicoll, S.B., Seyhan, S.L., Ateshian, G.A., and Hung, C.T. Synergistic action of growth factors and dynamic loading for articular cartilage tissue engineering. Tissue Eng **9,** 597, 2003.
34. Mauck, R.L., Soltz, M.A., Wang, C.C., Wong, D.D., Chao, P.H., Valhmu, W.B., Hung, C.T., and Ateshian, G.A. Functional tissue engineering of articular cartilage through dynamic loading of chondrocyte-seeded agarose gels. J Biomech Eng **122,** 252, 2000.
35. Nettles, D.L., Elder, S.H., and Gilbert, J.A. Potential use of chitosan as a cell scaffold material for cartilage tissue engineering. Tissue Eng **8,** 1009, 2002.
36. Cao, Y., Rodriguez, A., Vacanti, M., Ibarra, C., Arevalo, C., and Vacanti, C.A. Comparative study of the use of poly (glycolic acid), calcium alginate and pluronics in the engineering of autologous porcine cartilage. J Biomater Sci Polym Ed **9,** 475, 1998.
37. Chang, S.C., Rowley, J.A., Tobias, G., Genes, N.G., Roy, A.K., Mooney, D.J., Vacanti, C.A., and Bonassar, L.J. Injection molding of chondrocyte/alginate constructs in the shape of facial implants. J Biomed Mater Res **55,** 503, 2001.
38. Fragonas, E., Valente, M., Pozzi-Mucelli, M., Toffanin, R., Rizzo, R., Silvestri, F., and Vittur, F. Articular cartilage repair in rabbits by using suspensions of allogenic chondrocytes in alginate. Biomaterials **21,** 795, 2000.
39. Kuo, C.K., and Ma, P.X. Maintaining dimensions and mechanical properties of ionically crosslinked alginate hydrogel scaffolds *in vitro*. J Biomed Mater Res A **84A,** 899, 2007.
40. LeRoux, M.A., Guilak, F., and Setton, L.A. Compressive and shear properties of alginate gel: effects of sodium ions and alginate concentration. J Biomed Mater Res **47,** 46, 1999.
41. Hendrickson, D.A., Nixon, A.J., Grande, D.A., Todhunter, R.J., Minor, R.M., Erb, H., and Lust, G. Chondrocyte-fibrin matrix transplants for resurfacing extensive articular cartilage defects. J Orthop Res **12,** 485, 1994.
42. Kurz, B., Domm, C., Jin, M., Sellckau, R., and Schunke, M. Tissue engineering of articular cartilage under the influence of collagen I/III membranes and low oxygen tension. Tissue Eng **10,** 1277, 2004.
43. Dausse, Y., Grossin, L., Miralles, G., Pelletier, S., Mainard, D., Hubert, P., Baptiste, D., Gillet, P., Dellacherie, E., Netter, P., and Payan, E. Cartilage repair using new polysaccharidic biomaterials: macroscopic, histological and biochemical approaches in a rat model of cartilage defect. Osteoarthritis Cartilage **11,** 16, 2003.
44. Aigner, J., Tegeler, J., Hutzler, P., Campoccia, D., Pavesio, A., Hammer, C., Kastenbauer, E., and Naumann, A. Cartilage tissue engineering with novel nonwoven structured biomaterial based on hyaluronic acid benzyl ester. J Biomed Mater Res **42,** 172, 1998.
45. Kang, Y., Yang, J., Khan, S., Anissian, L., and Ameer, G.A. A new biodegradable polyester elastomer for cartilage tissue engineering. J Biomed Mater Res A **77,** 331, 2006.
46. Bryant, S.J., and Anseth, K.S. Hydrogel properties influence ECM production by chondrocytes photoencapsulated in poly(ethylene glycol) hydrogels. J Biomed Mater Res **59,** 63, 2002.
47. Lee, W.K., Ichi, T., Ooya, T., Yamamoto, T., Katoh, M., and Yui, N. Novel poly(ethylene glycol) scaffolds crosslinked by hydrolyzable polyrotaxane for cartilage tissue engineering. J Biomed Mater Res A **67,** 1087, 2003.

48. Freed, L.E., Vunjak-Novakovic, G., and Langer, R. Cultivation of cell-polymer cartilage implants in bioreactors. J Cell Biochem **51,** 257, 1993.
49. Martin, I., Obradovic, B., Treppo, S., Grodzinsky, A.J., Langer, R., Freed, L.E., and Vunjak-Novakovic, G. Modulation of the mechanical properties of tissue engineered cartilage. Biorheology **37,** 141, 2000.
50. Wang, Y., Kim, U.J., Blasioli, D.J., Kim, H.J., and Kaplan, D.L. *In vitro* cartilage tissue engineering with 3D porous aqueous-derived silk scaffolds and mesenchymal stem cells. Biomaterials **26,** 7082, 2005.
51. Wayne, J.S., McDowell, C.L., Shields, K.J., and Tuan, R.S. *In vivo* response of polylactic acid-alginate scaffolds and bone marrow-derived cells for cartilage tissue engineering. Tissue Eng **11,** 953, 2005.
52. Wei, Y., Hu, Y., Hao, W., Han, Y., Meng, G., Zhang, D., Wu, Z., and Wang, H. A novel injectable scaffold for cartilage tissue engineering using adipose-derived adult stem cells. J Orthop Res **26,** 27, 2008.
53. Williams, C.G., Kim, T.K., Taboas, A., Malik, A., Manson, P., and Elisseeff, J. *In vitro* chondrogenesis of bone marrow-derived mesenchymal stem cells in a photopolymerizing hydrogel. Tissue Eng **9,** 679, 2003.
54. Gimble, J.M., and Guilak, F. Differentiation potential of adipose derived adult stem (ADAS) cells. Curr Top Dev Biol **58,** 137, 2003.
55. Aust, L., Devlin, B., Foster, S.J., Halvorsen, Y.D., Hicok, K., du Laney, T., Sen, A., Willingmyre, G.D., and Gimble, J.M. Yield of human adipose-derived adult stem cells from liposuction aspirates. Cytotherapy **6,** 7, 2004.
56. Estes, B.T., Wu, A.W., Storms, R.W., and Guilak, F. Extended passaging, but not aldehyde dehydrogenase activity, increases the chondrogenic potential of human adipose-derived adult stem cells. J Cell Physiol **209,** 987, 2006.
57. Guilak, F., Lott, K.E., Awad, H.A., Cao, Q., Hicok, K.C., Fermor, B., and Gimble, J.M. Clonal analysis of the differentiation potential of human adipose-derived adult stem cells. J Cell Physiol **206,** 229, 2006.
58. Erickson, G.R., Gimble, J.M., Franklin, D.M., Rice, H.E., Awad, H., and Guilak, F. Chondrogenic potential of adipose tissue-derived stromal cells *in vitro* and *in vivo*. Biochem Biophys Res Commun **290,** 763, 2002.
59. Estes, B.T., Wu, A.W., and Guilak, F. Potent induction of chondrocytic differentiation of human adipose-derived adult stem cells by bone morphogenetic protein 6. Arthritis Rheum **54,** 1222, 2006.
60. Hennig, T., Lorenz, H., Thiel, A., Goetzke, K., Dickhut, A., Geiger, F., and Richter, W. Reduced chondrogenic potential of adipose tissue derived stromal cells correlates with an altered TGFbeta receptor and BMP profile and is overcome by BMP-6. J Cell Physiol **211,** 682, 2007.
61. Hofmann, S., Knecht, S., Langer, R., Kaplan, D.L., Vunjak-Novakovic, G., Merkle, H.P., and Meinel, L. Cartilage-like tissue engineering using silk scaffolds and mesenchymal stem cells. Tissue Eng **12,** 2729, 2006.
62. Sheyn, D., Pelled, G., Zilberman, Y., Talasazan, F., Frank, J.M., Gazit, D., and Gazit, Z. Nonvirally engineered porcine adipose tissue-derived stem cells: use in posterior spinal fusion. Stem Cells **26,** 1056, 2008.
63. Huang, C.Y., Hagar, K.L., Frost, L.E., Sun, Y., and Cheung, H.S. Effects of cyclic compressive loading on chondrogenesis of rabbit bone-marrow derived mesenchymal stem cells. Stem Cells **22,** 313, 2004.
64. Mauck, R.L., Byers, B.A., Yuan, X., and Tuan, R.S. Regulation of cartilaginous ECM gene transcription by chondrocytes and MSCs in 3D culture in response to dynamic loading. Biomech Model Mechanobiol **6,** 113, 2007.
65. Awad, H.A., Wickham, M.Q., Leddy, H.A., Gimble, J.M., and Guilak, F. Chondrogenic differentiation of adipose-derived adult stem cells in agarose, alginate, and gelatin scaffolds. Biomaterials **25,** 3211, 2004.
66. Betre, H., Ong, S.R., Guilak, F., Chilkoti, A., Fermor, B., and Setton, L.A. Chondrocytic differentiation of human adipose-derived adult stem cells in elastin-like polypeptide. Biomaterials **27,** 91, 2006.
67. Kuo, C.K., Li, W.J., Mauck, R.L., and Tuan, R.S. Cartilage tissue engineering: its potential and uses. Curr Opin Rheumatol **18,** 64, 2006.
68. Urist, M.R. Bone: formation by autoinduction. Science **150,** 893, 1965.
69. Mow, V.C., and Lai, W.M. Recent developments in synovial joint biomechanics. SIAM Rev **22,** 275, 1980.
70. Kim, U.J., Park, J., Kim, H.J., Wada, M., and Kaplan, D.L. Three-dimensional aqueous-derived biomaterial scaffolds from silk fibroin. Biomaterials **26,** 2775, 2005.
71. Mehlhorn, A.T., Niemeyer, P., Kaiser, S., Finkenzeller, G., Stark, G.B., Sudkamp, N.P., and Schmal, H. Differential expression pattern of extracellular matrix molecules during chondrogenesis of mesenchymal stem cells from bone marrow and adipose tissue. Tissue Eng **12,** 2853, 2006.
72. Farndale, R.W., Buttle, D.J., and Barrett, A.J. Improved quantitation and discrimination of sulphated glycosaminoglycans by use of dimethylmethylene blue. Biochim Biophys Acta **883,** 173, 1986.
73. Woessner, J.F., Jr. The determination of hydroxyproline in tissue and protein samples containing small proportions of this imino acid. Arch Biochem Biophys **93,** 440, 1961.
74. Mow, V.C., Kuei, S.C., Lai, W.M., and Armstrong, C.G. Biphasic creep and stress-relaxation of articular-cartilage in compression—theory and experiments. J Biomech Eng (Transactions of the Asme) **102,** 73, 1980.
75. Hasslund, S., Jacobson, J.A., Dadali, T., Basile, P., Ulrich-Vinther, M., Soballe, K., Schwarz, E.M., O'Keefe, R.J., Mitten, D.J., and Awad, H.A. Adhesions in a murine flexor tendon graft model: autograft versus allograft reconstruction. J Orthop Res **26,** 824, 2008.
76. Basile, P., Dadali, T., Jacobson, J., Hasslund, S., Ulrich-Vinther, M., Soballe, K., Nishio, Y., Drissi, M.H., Langstein, H.N., Mitten, D.J., O'Keefe, R.J., Schwarz, E.M., and Awad, H.A. Freeze-dried Tendon allografts as tissue-engineering scaffolds for Gdf5 gene delivery. Mol Ther **16,** 466, 2008.
77. Chun, S.Y., Lim, G.J., Kwon, T.G., Kwak, E.K., Kim, B.W., Atala, A., and Yoo, J.J. Identification and characterization of bioactive factors in bladder submucosa matrix. Biomaterials **28,** 4251, 2007.
78. Gilbert, T.W., Sellaro, T.L., and Badylak, S.F. Decellularization of tissues and organs. Biomaterials **27,** 3675, 2006.
79. Ott, H.C., Matthiesen, T.S., Goh, S.K., Black, L.D., Kren, S.M., Netoff, T.I., and Taylor, D.A. Perfusion-decellularized matrix: using nature's platform to engineer a bioartificial heart. Nat Med **14,** 213, 2008.
80. Wilshaw, S.P., Kearney, J.N., Fisher, J., and Ingham, E. Production of an acellular amniotic membrane matrix for use in tissue engineering. Tissue Eng **12,** 2117, 2006.
81. Xu, C.C., Chan, R.W., and Tirunagari, N. A biodegradable, acellular xenogeneic scaffold for regeneration of the vocal fold lamina propria. Tissue Eng **13,** 551, 2007.

82. Toolan, B.C., Frenkel, S.R., Pereira, D.S., and Alexander, H. Development of a novel osteochondral graft for cartilage repair. J Biomed Mater Res **41,** 244, 1998.
83. Ng, K.W., Defrancis, J.G., Kugler, L.E., Kelly, T.A., Ho, M.M., O'Conor, C.J., Ateshian, G.A., and Hung, C.T. Amino acids supply in culture media is not a limiting factor in the matrix synthesis of engineered cartilage tissue. Amino Acids **35,** 433, 2007.
84. Eyre, D.R., McDevitt, C.A., Billingham, M.E., and Muir, H. Biosynthesis of collagen and other matrix proteins by articular cartilage in experimental osteoarthrosis. Biochem J **188,** 823, 1980.
85. Guilak, F., Butler, D.L., and Goldstein, S.A. Functional tissue engineering: the role of biomechanics in articular cartilage repair. Clin Orthop Relat Res **391 (suppl),** S295, 2001.
86. Athanasiou, K.A., Rosenwasser, M.P., Buckwalter, J.A., Malinin, T.I., and Mow, V.C. Interspecies comparisons of *in situ* intrinsic mechanical properties of distal femoral cartilage. J Orthop Res **9,** 330, 1991.
87. Mauck, R.L., Wang, C.C., Oswald, E.S., Ateshian, G.A., and Hung, C.T. The role of cell seeding density and nutrient supply for articular cartilage tissue engineering with deformational loading. Osteoarthritis Cartilage **11,** 879, 2003.
88. Mauck, R.L., Yuan, X., and Tuan, R.S. Chondrogenic differentiation and functional maturation of bovine mesenchymal stem cells in long-term agarose culture. Osteoarthritis Cartilage **14,** 179, 2006.
89. Armstrong, C.G., and Mow, V.C. Variations in the intrinsic mechanical properties of human articular cartilage with age, degeneration, and water content. J Bone Joint Surg Am **64,** 88, 1982.
90. Guilak, F., Awad, H.A., Fermor, B., Leddy, H.A., and Gimble, J.M. Adipose-derived adult stem cells for cartilage tissue engineering. Biorheology **41,** 389, 2004.
91. Awad, H.A., Halvorsen, Y.D., Gimble, J.M., and Guilak, F. Effects of transforming growth factor beta1 and dexamethasone on the growth and chondrogenic differentiation of adipose-derived stromal cells. Tissue Eng **9,** 1301, 2003.
92. Cardone, M.H., Salvesen, G.S., Widmann, C., Johnson, G., and Frisch, S.M. The regulation of anoikis: MEKK-1 activation requires cleavage by caspases. Cell **90,** 315, 1997.
93. Frisch, S.M., and Francis, H. Disruption of epithelial cell-matrix interactions induces apoptosis. J Cell Biol **124,** 619, 1994.
94. Shakibaei, M. Inhibition of chondrogenesis by integrin antibody *in vitro*. Exp Cell Res **240,** 95, 1998.
95. Larson, C.M., Kelley, S.S., Blackwood, A.D., Banes, A.J., and Lee, G.M. Retention of the native chondrocyte pericellular matrix results in significantly improved matrix production. Matrix Biol **21,** 349, 2002.
96. Bosnakovski, D., Mizuno, M., Kim, G., Takagi, S., Okumura, M., and Fujinaga, T. Chondrogenic differentiation of bovine bone marrow mesenchymal stem cells (MSCs) in different hydrogels: influence of collagen type II extracellular matrix on MSC chondrogenesis. Biotechnol Bioeng **93,** 1152, 2006.
97. Maquart, F.X., Pasco, S., Ramont, L., Hornebeck, W., and Monboisse, J.C. An introduction to matrikines: extracellular matrix-derived peptides which regulate cell activity. Implication in tumor invasion. Crit Rev Oncol Hematol **49,** 199, 2004.
98. Murugan, R., Ramakrishna, S., and Rao, K.P. Analysis of bovine-derived demineralized bone extracts. J Mater Sci Mater Med **19,** 2423, 2008.
99. Ahmed, N., Dreier, R., Gopferich, A., Grifka, J., and Grassel, S. Soluble signalling factors derived from differentiated cartilage tissue affect chondrogenic differentiation of rat adult marrow stromal cells. Cell Physiol Biochem **20,** 665, 2007.

Address reprint requests to:
Farshid Guilak, Ph.D.
Orthopaedic Research Laboratories
Division of Orthopaedic Surgery
Department of Surgery
Duke University Medical Center
375 MSRB, Box 3093
Durham, NC 27710

E-mail: guilak@duke.edu

Received: April 28, 2008
Accepted: August 25, 2008
Online Publication Date: October 24, 2008